2015

Endoplasmic Reticulum - Mitochondrial Interactions in House Dust Mite Induced Inflammation

Jonathon M. Cahoon
University of Vermont, jcahoon@uvm.edu

Vikas Anathy
University of Vermont, vikas.anathy@med.uvm.edu

Endoplasmic Reticulum – Mitochondrial Interactions in House Dust Mite Induced Inflammation

Thesis submitted to University of Vermont College of Arts and Sciences for The College Honors Program

by

Jonathon M. Cahoon

Department of Biology
College of Arts and Sciences
University of Vermont
Burlington, VT, 05405

April 2015

Abstract

Rationale: Airway epithelial cells (AECs) are critical regulators of inflammatory, immune and injury responses to allergens that contribute to asthma pathogenesis. The response of AECs to allergens requires an integrated-complex, extracellular receptors and intracellular organelle interaction to achieve secretion of pro-inflammatory cytokines and chemokines. Endoplasmic reticulum (ER) and mitochondria interactions have previously been shown to induce mitochondrial fission. Mitochondrial fission may be a key parameter allergen induced airway inflammation in asthma. However, ER-mitochondria interactions, mitochondrial fission, and subsequent production and secretion of cytokines and chemokines in response to House Dust Mite (HDM) are not well understood.

Objective: Here we will assess the ability of HDM to induce ER-mitochondrial interactions and subsequent mitochondrial fission in human bronchiolar epithelial (HBE) cells. We will also investigate the impact on cytokine production downstream of mitochondrial fission in HBE cells treated with HDM.

Methods: ER-mitochondrial interactions were quantified using confocal and epifluorescence microscopy. Cytokine/chemokine profiles were determined by enzyme linked immunosorbant assay (ELISA) using HBE cells treated with HDM.

Measurements and Main Results: Using epifluorescence and confocal microscopy we show that ER-mitochondrial contacts are increased in response to HDM treatment, as well as HDM-induced mitochondrial fission increased in HBE cells. Inhibition of DRP1, a protein essential for mitochondrial fission, decreases HDM induced ER-mitochondrial interaction. In addition, HDM-induced pro-inflammatory cytokines were decreased in HBE cells where mitochondrial fission is inhibited.

Conclusion: HDM induces ER-Mitochondrial interactions that promote mitochondrial fission and subsequent production of pro-inflammatory cytokines.

Introduction

Under normal physiological conditions the endoplasmic reticulum (ER) is responsible for the proper folding of proteins. An increase in the physiological demand for protein folding can lead to an increase in misfolded proteins in the ER[1]. This is a result of an imbalance in synthesis of proteins and the ER's capacity to fold these proteins. The increased amount of misfolded proteins leads to the ER stress response, which induces a physiological change to the ER and ultimately leads to cell death [2].

The ER stress response induces reorganization of the ER membrane as well as promotes morphological changes in the ER [3]. Along with this reorganization the stress response induces the unfolded protein response (UPR). The UPR signals the ER to expand by generation of ER sheets [4]. However, the expansion of the ER without the UPR has also shown alleviation of the ER stress response, which indicates ER size is a key factor of a cell's ability to cope with ER stress [5]. The change in ER morphology and its increase in size leads to increased interorganelle cross-talk between the ER and mitochondria [6-8]. This cross-talk has been observed to mark the sites of mitochondrial fission, specifically at the site where ER tubules contacted the mitochondria [9].

Mitochondrial fission has previously been associated with inflammation in airway smooth muscle cells and astrocytes [10, 11]. Fission of the mitochondria is largely regulated by dynamin related protein 1 (DRP1), which induces contraction of the mitochondrial membrane [12]. When DRP1 is recruited to the mitochondrial membrane it assembles into ring-like multimers around the outer mitochondrial membrane and constricts to cause fission [9, 12-15]. DRP1 activity is primarily regulated through phosphorylation, specifically at Ser616 [12, 16, 17]. When ER stress causes expansion of

the ER its tubules contact the mitochondria [7, 8]. Initial constriction of the mitochondrial membrane starts at these contact sites followed by heavy recruitment of DRP1 and ultimately mitochondrial fission [9, 14].

House Dust Mite (HDM) is one of the most commonly found airborne allergens and induces an allergic response in many asthmatics [18]. HDM has been shown to cause the ER stress response in airway epithelial cells, which ultimately leads to inflammation, apoptosis, bronchiolar fibrosis, and airway hyperresponsiveness [19]. The goals of this study were to determine 1) the extent of ER - mitochondrial interactions in response to HDM; 2) if these interactions induce mitochondrial fission through promotion of DRP1 recruitment to the mitochondrial membrane; and 3) whether the pro-inflammatory response to HDM can be diminished by reducing mitochondrial fission by disrupting DRP1 function.

Methods

Cell Culture

A human bronchiolar epithelial (HBE) cell line was provided by Rean Wu, UC Davis.

Growth Media: The HBE cells were grown in DMEM/F12 media (Gibco) containing final concentrations of 50 units/mL penicillin and 50 µg/mL streptomycin, 10 ng/mL cholera toxin, 10 ng/mL epidermal growth factor, 5 µg/mL insulin, 5 µg/mL transferrin, 0.1µM dexamethasone, 15 µg/mL bovine pituitary extract, and 0.5 mg/mL bovine serum albumin.

Propagation: When cells were 100% confluent media was removed and cells were treated with trypsin. After about 10 minutes, cells are rounded and detached when

viewed under a microscope, Fetal Bovine Serum (FBS) was added to halt the trypsin reaction. Cells were pelleted by centrifugation and the supernatant was removed. the cells were then resuspended in growth media. The cells were passed to a fresh flask and fresh growth media was added.

Transfection: Cells were cultured with an initial concentration of $1.5x10^5$ cells in 35mm dishes (Mattek) containing 10mm coverslip inserts one day prior to transfection. Media was removed and replaced with 1mL of Opti-mem® reduced serum media (Gibco). Solutions containing 0.6µg of total plasmids in 250µL Opti-mem media combined with 7µL Lipofectimine® 3000 Reagent (Invitrogen) in 250µL Opti-mem media were prepared for each dish (e.g. cells transfected with dsRed, Sec61b, and dnDRP1 would have 0.2µg of each plasmid in 250µL Opti-mem media). Solutions were incubated for 15 minutes at room temperature. 500µL of plasmid solutions were added to each dish, without removing the media already in the dishes, and incubated for 4 hours at 37°C. Opti-mem media was then removed and replaced by growth media. Cells were incubated at 37°C overnight and harvested or imaged the following day.

Treatment and harvesting: HBE cells were exposed to either phosphate buffered saline (PBS) or 50µg HDM. Cells were starved in growth factor media for 1 hour prior to treatment. At various time points supernatant from cells were collected and frozen. Cells were then lysed in buffer containing 137mM Tris•HCl (pH 8.0), 130 mM NaCl, and 1% NP-40 with phosphatase and protease inhibitors. Cells were immediately collected and frozen after being lysed.

Western Blot

Cell lysate from harvested cells was thawed. Insoluble proteins were pelleted via centrifugation at 18000 g for 10 minutes at 4°C and protein quantitation of the supernatant was performed using the Lowrey method (DC Protein Assay, BioRad Laboratories, Hercules, CA). Protein lysate (50μg) was then resuspended in loading buffer with dithiothrietal (DTT) and resolved by SDS-PAGE using 12% polyacrylamide gels. Proteins were transferred onto PVDF membranes and were probed using a standard immunoblotting protocol using the following primary antibodies: phospho-DRP1 (S616) (1:1000, rabbit), total DRP1 (1:1000, rabbit), β –Actin (1:3000, mouse).

Cytokine Profiling

Cells ($1.5x10^5$) were plated and transfected with either pcDNA3, a control plasmid, or dominant negative dynamin related protein 1 (dnDRP1), which prevents oligomerization of DRP1 and inhibits subsequent mitochondrial fission, plasmids. Cells were challenged with HDM, harvested, and then frozen as previously described. Supernatant from harvested cells were thawed and assayed for pro-inflammatory cytokine and chemokine levels by enzyme linked immunosorbant assay (ELISA) (Duoset ELISA, R&D Systems, Minneapolis, MN) per the manufacturer's instructions.

Capture antibody was diluted to the working concentration in PBS. A 96-well microplate was coated with 100 μL per well of diluted capture antibody. The plate was sealed and incubated overnight at ambient temperature or 2 hours at 37°C. Each well was then washed three times with wash-buffer (0.05% Tween® 20 in PBS) using a squirt bottle. After the last wash the plate was inverted and blotted against clean paper towels to

completely remove any remaining wash-buffer. Non-specific binding sites were then blocked with 200 µL of Reagent Diluent (1% BSA in PBS) for a minimum of 1 hour at ambient temperature. The plates were washed as previously described.

Standards in Reagent Diluent or cell supernatant (100µL) were loaded into wells. The plate was then sealed and incubated overnight at 4°C. The plate was washed as previously described. Detection antibody (100µL), diluted in Reagent Diluent, was added to each well. The plate was sealed and incubated for 2 hours at ambient temperature. The plate was washed as previously described. Streptavidin-HRP (100µL), diluted at 1:200 in 1% BSA in PBS, was added to each well. The plate was sealed and incubated in the dark for 20 minutes at ambient temperature. The plate was washed as previously described. Substrate Solution (100µL of 1:1 mixture H_2O_2 and Tetramethylbenzidine) was added to each well and incubated at room temperature for 20 minutes in the dark. Stop Solution (50µL of 2N H_2SO_4) was added to every well. The optical density (OD) of each well was immediately determined using a PowerWave (Bio-Tek Instruments) set to 450nm and 570nm. Readings from 570nm were subtracted from reading at 450nm to correct for optical imperfections in the plate.

Cell Imaging

Cells ($1.5x10^5$) were placed in 35mm dishes (Mattek) with 10mm coverslips and transfected with plasmids expressing mitochondrial specific red fluorescent (Mito DsRed) protein and ER specific green or turquoise fluorescent (GFP-Sec61b or ER-turq) protein. Cells were also transfected with either pcDNA3 or dnDRP1. Imaging began immediately after treatment of either PBS or HDM. Three groups of 4-7 cells from each

plate were imaged for 20 minutes each at 30-second intervals in a single focal plane with or without HDM. Images were captured with the Zeiss LSM 510 META Confocal Laser Scanning Imaging System with excitation wavelengths at 488 and 543 nm at 40X water immersion. Alternatively a group of cells was imaged for 80 minutes at 2 minute intervals in a single focal plane after HDM treatment. Images were captured using an inverted epi-fluorescence microscope (TE2000-U; Nikon) at 100X.

Alternatively, paraffin-embedded slides from mice challenged with HDM or PBS (vehicle control) were prepared for immunofluorescence. The lung-tissue samples on the slides were deparaffinized. Antigens were exposed by extraction in Citrate Buffer at 95°C for 20 minutes then cooled at ambient temperature for 20 minutes. Slides were then blocked with 5% BSA in PBS for a minimum of 1 hour followed by incubation with DRP1 (1:500, rabbit) or phospho-DRP1 (S616) (1:500, rabbit) primary antibodies overnight at 4°C. Slides were then washed in PBS and the secondary fluorescent antibody (Alexafluor 647 1:1000, rabbit) was added for 1 hour in the dark at ambient temperature. Slides were then washed in PBS followed by incubation of DAPI (1:4000) for 10 minutes in the dark at ambient temperature. The slides were washed, coverslipped, and mounted. Slides were imaged with the Zeiss LSM 510 META Confocal Laser Scanning Imaging System at 40X oil immersion with excitation wavelengths at 633 nm.

Volocity software was used determine the Mander's Colocalization Coefficient (MCC), specifically M1 and M2 Colocalization Coefficients, for the ER and mitochondria interactions. Metamorph software was utilized to measure mitochondrial length using the line tool. Mitochondrial length and branching will also be measured by mitochondrial form factor using the formula $ff = (perimeter^2)/(4\pi*area)$. As per the

convention only peripheral regions of the cell, where contacts between ER and mitochondria or mitochondrial structure were well resolved, were subjected to analysis [20].

Statistics

Data from total of three experiments were averaged and expressed as mean values ± standard errors of the means (SEM). Data was analyzed by nonparametric t-test or one-way analysis of variance (ANOVA), with the Tukey test for multiple comparisons wherever necessary. Results at $P < 0.05$ were considered statistically significant.

Results

ER-Mitochondrial interactions are increased in HDM challenged HBE cells.

Cells grown on coverslips were transfected with Mito-dsred and ER-turquoise and challenged with HDM. Images acquired from the epi-fluorescent microscope show mitochondrial length decreasing as well as increased amount of ER-mitochondrial co-occurrence. ER (blue) and mitochondrial (red) contacts significantly increased ($p<0.01$) at 40 minutes after HDM challenge in HBE cells (Figure 1A,B).

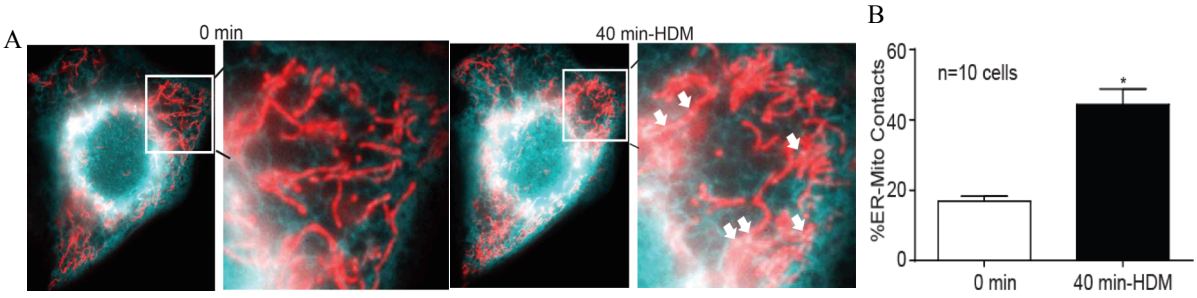

HDM increase ER-mitochondrial contacts 40 minutes after treatment in HBE cells.
Fig 1. A: Representative images of ER (blue) and mitochondrial (red) contact sites in HDM stimulated HBE cells (arrows). **B:** Quantitation by counting mitochondria overlapping with ER in HDM stimulated cells at 0 minutes and 40 minutes (*$p<0.01$).

DnDRP1 decreases ER-Mitochondrial interactions in HDM challenged HBE cells.

Cells transfected with pcDNA or dnDRP1 were challenged with HDM then imaged for one hour with the Zeiss LSM 510 META Confocal Laser Scanning Imaging System. Images were quantified using Volocity software for Mander's Colocalization Coefficient to determine the ER (green) – mitochondria (red) interactions (Figure 2C,E).

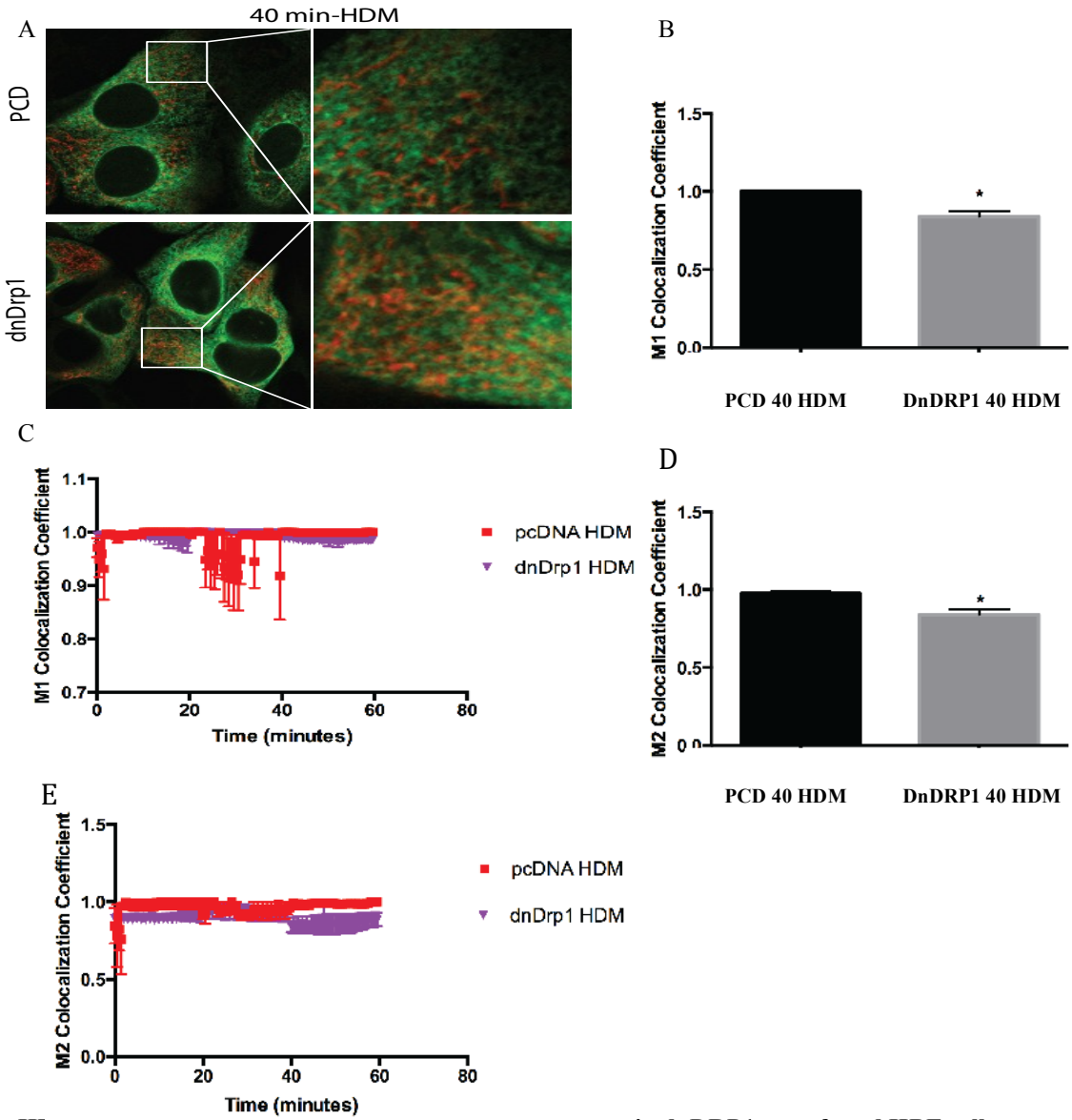

HDM induced ER-Mitochondrial interactions decreased in dnDRP1 transfected HBE cells.

Fig 2. A: Representative images of ER (green) and mitochondria (red) interactions in HDM challenged HBE cells. Boxes are representative of areas used for Mander's or Pearson's Cololalization analysis (areas were selected using a freehand selection tool). **B:** Quantitation of ER - mitochondrial contacts by M1 (Mander's Green-Red) Colocalization Coefficient in HBE cells at 40 minutes after HDM treatment (*p<0.05) **C:** M1 Correlation Coefficient between HDM treated HBE cells. **D:** Quantitation of ER – mitochondrial contacts by M2 (Mander's Red-Green) Colocalization Coefficient in HBE cells at 40 minutes after HDM treatment (*p<0.05). **E:** M2 Colocalization Coefficient in HDM treated HBE cells.

Cells transfected with dnDRP1 showed fewer ER-mitochondria interactions when compared to pcDNA-transfected cells at 40 minutes after HDM treatment (n=30, $p<0.05$)(Figure 2B,D).

Mitochondrial fission increases in HDM treated HBE cells.

HBE cells transfected with pcDNA or dnDrp1 were treated with HDM and imaged every 2 minutes for 80 minutes using confocal microscopy. Mitochondrial networking quantification by form factor calculations show mitochondria have significantly decreased networking in HBE cells at the 80 minute mark after HDM challenge as compared to their control counterparts (n=50, $p<0.001$) (Figure 3A). The decreased mitochondrial networking is associated with an increase in phosphorylation of

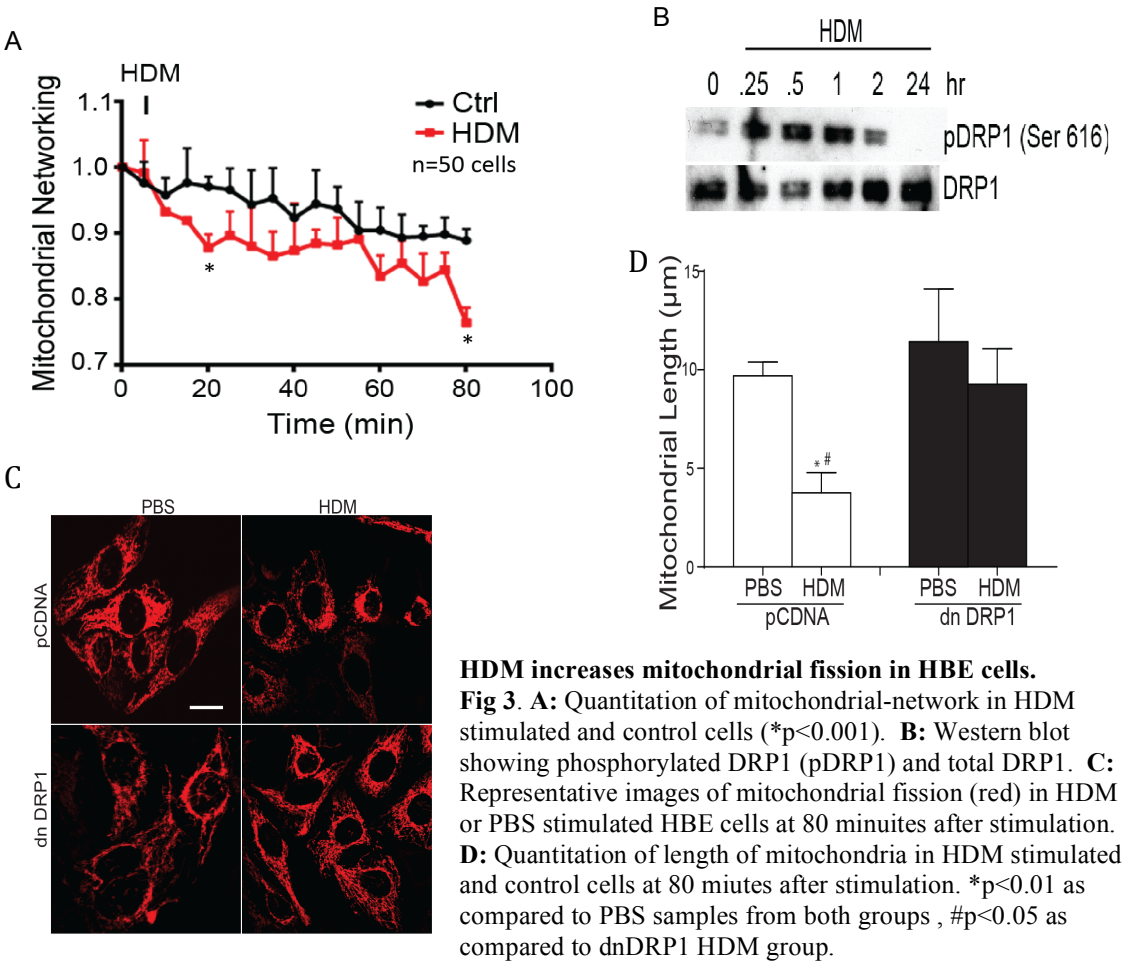

HDM increases mitochondrial fission in HBE cells.
Fig 3. **A:** Quantitation of mitochondrial-network in HDM stimulated and control cells (*$p<0.001$). **B:** Western blot showing phosphorylated DRP1 (pDRP1) and total DRP1. **C:** Representative images of mitochondrial fission (red) in HDM or PBS stimulated HBE cells at 80 minuites after stimulation. **D:** Quantitation of length of mitochondria in HDM stimulated and control cells at 80 miutes after stimulation. *$p<0.01$ as compared to PBS samples from both groups , #$p<0.05$ as compared to dnDRP1 HDM group.

DRP1 at the activating serine 616 (Figure 3B). Mitochondria (red) show increased fragmentation in cells exposed to HDM and transfected with pcDNA (Figure 3C). Quantitation of mitochondrial length, using the line tool of MetaMorph image analysis software, shows cells transfected with pcDNA and treated with HDM had decreased mitochondrial length as compared to their PBS treated counterparts ($p<0.01$), as well as when compared to cells transfected with dnDRP1 and challenged with HDM ($p<0.05$) (Figure 3D).

DndDRP1 decreases pro-inflammatory cytokine production.

Chemokine interleukin 8 (IL-8), a key parameter for activation, degranulation, and chemotaxis of neutrophils into inflamed tissues [21], showed a decrease in cells transfected with dnDRP1 at 24 hours ($p<0.0001$) and 48 hours ($p<0.0001$) when compared to cells transfected with pcDNA (Figure 4A). Interleukin1-beta (IL-1β), a primary cytokine involved with inflammation [22], also showed a decrease in cells transfected with dnDRP1 at 24 hours ($p<0.0001$) and 48 hours ($p<0.0001$) when compared to cells transfected with pcDNA (Figure 4B).

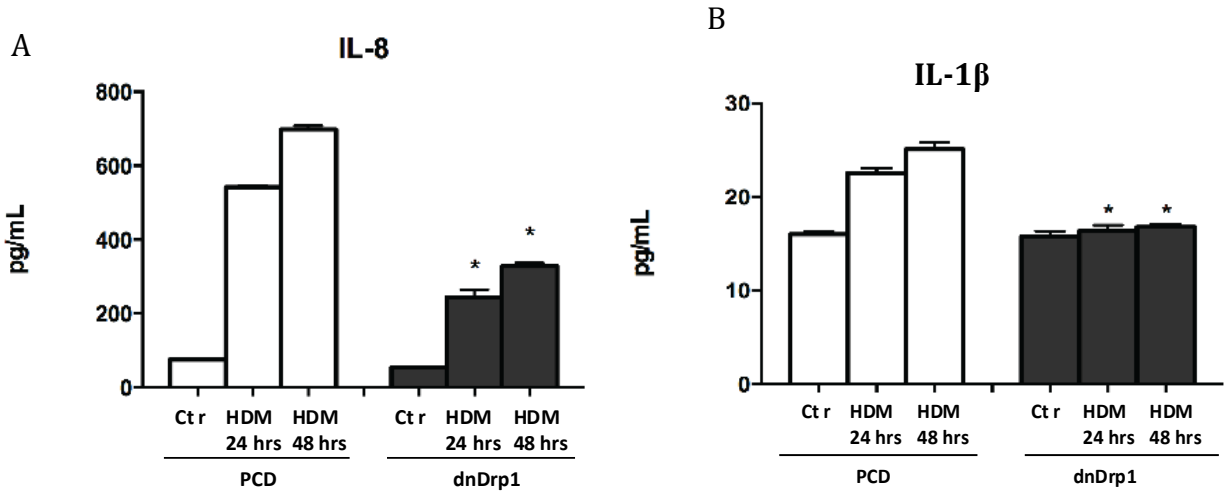

HDM induced Pro-inflammatory cytokine production is attenuated by dnDRP1 transfection in HBE cells.
Fig 4 Pro-inflammatory chemokine IL-8 (**A**) and cytokine IL-1β (**B**) in HBE cells transfected with PCD or

Phosphorylation of DRP1 increases in lung tissue from mice treated with HDM.

DRP1 is activated via phosphorylation of serine 616 and promotes mitochondrial fission [16, 17]. To assess HDM-induced DRP1 activation, paraffin embedded slides from wild type mice treated with either PBS or HDM were prepared for immunofluorescence for DRP1 and phospho-DRP1 (S616). Mice treated with HDM had more phospho-DRP1 in lung tissue, most notably in airway epithelial cells, when compared to their PBS counterparts. Overall DRP1 was relatively the same between HDM and PBS treated groups (Figure 5).

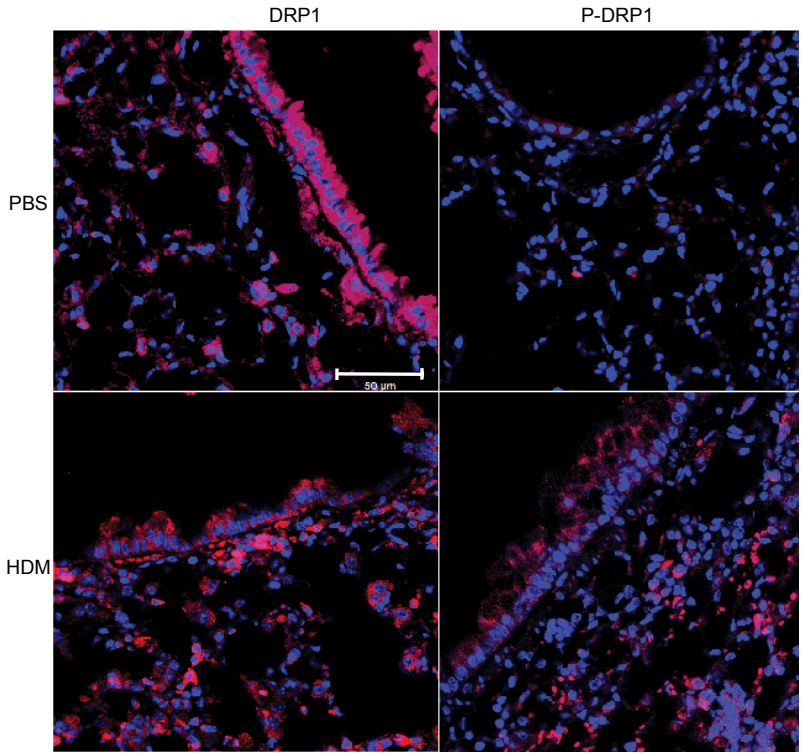

DRP1 phosphorylation increases in lung tissue from mice treated with HDM.

Figure 5. Representative images of DRP1 and p-DRP1 in mice challenged with HDM or PBS. Phosphorylation of DRP1 is increased in tissue from mice treated with HDM.

Discussion

ER stress occurs when an imbalance exists between the synthesis of proteins and the ER's capacity to fold these proteins. This response by the cell is a mechanism to repair misfolded proteins during physiological stress [23]. HDM has previously been shown to activate the ER stress pathway [19] and this stress on the ER is known to induce an inflammatory response in airways [19, 24]. Previous studies have found ER stress leads to expansion of the ER and increases the amount of ER-mitochondrial contacts [7, 8], however allergen mediated ER-mitochondrial contacts is unknown. Our results suggest that HBE cells treated with HDM have a significant increase in the inter-organelle crosstalk between the ER and mitochondria around the 40-minute mark. ER-mitochondrial contacts are known to mark sites of mitochondrial fission in homeostatically proliferating cells [9, 14]. Our work shows HDM-induced increased contacts are associated with mitochondrial fission.

It is well known that ER-mitochondrial interactions and phosphorylation of DRP1 are very critical for ER mediated mitochondrial fission [9, 14]. We found that increases in ER-mitochondrial contacts were also associated with increases in phosphorylation of DRP1. Interestingly, HDM challenged lungs of mice also showed increases in phosphorylation of DRP1, indicating that DRP1 phosphorylation may play a causal role in allergen-induced pro-inflammatory response.

Mitochondria morphology changes dynamically through fission and fusion events critical for maintaining cellular homeostasis [12, 15]. It is known that the dominant negative form of DRP1 (dnDRP1 K38E) disrupts oligomerization of DRP1 on the mitochondria, thus decreasing fission of mitochondria [14, 25]. Our experiments showed

that ectopic expression of dnDRP1 not only decreased HDM-induced ER-mitochondrial contacts, but also fission of mitochondria, indicating a critical role for DRP1 in HDM-induced ER-mitochondrial interactions and fission events.

HDM, a common aeroallergen, is known to cause an inflammatory response in airway epithelial cells [18, 19]. Pro-inflammatory responses have previously been associated with both ER stress response [19] and mitochondrial fission when induced by other agents [10, 11]. Our data show that when DRP1 function is inhibited, by transfection of HBE cells with dnDRP1, mitochondrial fission is reduced. This reduction in mitochondrial fission is associated with a significant decrease in pro-inflammatory cytokine and chemokine levels. These results are indicative of mitochondrial fission being a key parameter in an inflammatory response to allergens in airway epithelial cells. Future experiments are needed to prove that HDM-induces fission events occur at the ER-mitochondrial contact sites in HBE cells.

Collectively our data show that HDM induces ER-mitochondrial interactions. These interactions are also associated with phosphorylation of DRP1 and subsequent mitochondrial fission. The HDM-induced a pro-inflammatory response seems to be downstream of mitochondrial fission. We have shown a novel pathway in which HDM induces a pro-inflammatory response through ER-mitochondrial interactions and DRP1 dependent mitochondrial fission.

Future Directions

In the future we would like to use STORM super resolution microscope system as well as an electron microscope to increase resolution of the cell imaging. These

microscopy techniques would allow us to perform a proof of concept experiment to resolve HDM-induced ER-mitocondrial contacts. Furthermore these additional microscopy techniques will allow us to see mitochondrial fission sites to confirm and demonstrate that fission occurs at the ER-mitochondrial contacts in response to HDM treatment. Additional experiments *in vivo* with $DRP1^{loxp/loxp}$ allele mice capable of deleting DRP1, specifically in epithelial cells, would further solidify data we have obtained; showing a decrease in inflammation when DRP1 function is inhibited along with translation of results from *in vitro* to *in vivo*.

We would also like to rectify technical difficulties that occurred during the limited time for this study. These factors include: limited access to microscopes with deconvolution and drift correction software, as well as difficulty in determining an appropriate threshold value representing background noise of images subject to Mander's Colocalization Coefficient. We believe the microscopy techniques described above will increase resolution of images obtained and decrease or eliminate the need for deconvolution software. Further collaboration with the University of Vermont Microscopy Imaging Center will better our techniques in obtaining clearer images and allow us to improve the analytical techniques, such as determining the background noise of images.

Acknowledgements

I thank my thesis advisor, Vikas Anathy, for his guidance and countless hours put into my learning. Thanks also to Sidra Hoffman, who patiently taught me many of the protocols and lab procedures. Thanks to the members my thesis defense committee,

Christopher Landry, Beth Bouchard, and Douglas Taatjes. I thank Nicole Bouffard, for training and help with imaging and image analysis. Funding for this research was provided by American Thoracic Society, University of Vermont College of Medicine Internal Grant Program, and NIHRO1HL122383 to Vikas Anathy.

References

1. Tabas, I. and D. Ron, *Integrating the mechanisms of apoptosis induced by endoplasmic reticulum stress.* Nat Cell Biol, 2011. **13**(3): p. 184-90.
2. Szegezdi, E., et al., *Mediators of endoplasmic reticulum stress-induced apoptosis.* EMBO Rep, 2006. **7**(9): p. 880-5.
3. Varadarajan, S., et al., *A novel cellular stress response characterised by a rapid reorganisation of membranes of the endoplasmic reticulum.* Cell Death Differ, 2012. **19**(12): p. 1896-907.
4. Schroder, M. and R.J. Kaufman, *ER stress and the unfolded protein response.* Mutat Res, 2005. **569**(1-2): p. 29-63.
5. Schuck, S., et al., *Membrane expansion alleviates endoplasmic reticulum stress independently of the unfolded protein response.* J Cell Biol, 2009. **187**(4): p. 525-36.
6. Wikstrom, J.D., et al., *AMPK regulates ER morphology and function in stressed pancreatic beta-cells via phosphorylation of DRP1.* Mol Endocrinol, 2013. **27**(10): p. 1706-23.
7. Bravo, R., et al., *Increased ER-mitochondrial coupling promotes mitochondrial respiration and bioenergetics during early phases of ER stress.* J Cell Sci, 2011. **124**(Pt 13): p. 2143-52.
8. Vannuvel, K., et al., *Functional and morphological impact of ER stress on mitochondria.* J Cell Physiol, 2013. **228**(9): p. 1802-18.
9. Friedman, J.R., et al., *ER tubules mark sites of mitochondrial division.* Science, 2011. **334**(6054): p. 358-62.
10. Aravamudan, B., et al., *Cigarette smoke-induced mitochondrial fragmentation and dysfunction in human airway smooth muscle.* Am J Physiol Lung Cell Mol Physiol, 2014. **306**(9): p. L840-54.
11. Motori, E., et al., *Inflammation-induced alteration of astrocyte mitochondrial dynamics requires autophagy for mitochondrial network maintenance.* Cell Metab, 2013. **18**(6): p. 844-59.
12. Otera, H., N. Ishihara, and K. Mihara, *New insights into the function and regulation of mitochondrial fission.* Biochim Biophys Acta, 2013. **1833**(5): p. 1256-68.
13. Smirnova, E., et al., *Dynamin-related protein Drp1 is required for mitochondrial division in mammalian cells.* Mol Biol Cell, 2001. **12**(8): p. 2245-56.
14. Korobova, F., V. Ramabhadran, and H.N. Higgs, *An actin-dependent step in mitochondrial fission mediated by the ER-associated formin INF2.* Science, 2013. **339**(6118): p. 464-7.
15. Youle, R.J. and A.M. van der Bliek, *Mitochondrial fission, fusion, and stress.* Science, 2012. **337**(6098): p. 1062-5.
16. Cribbs, J.T. and S. Strack, *Reversible phosphorylation of Drp1 by cyclic AMP-dependent protein kinase and calcineurin regulates mitochondrial fission and cell death.* EMBO Rep, 2007. **8**(10): p. 939-44.
17. Hong, Z., et al., *Role of dynamin-related protein 1 (Drp1)-mediated mitochondrial fission in oxygen sensing and constriction of the ductus arteriosus.* Circ Res, 2013. **112**(5): p. 802-15.

18. Gregory, L.G. and C.M. Lloyd, *Orchestrating house dust mite-associated allergy in the lung.* Trends Immunol, 2011. **32**(9): p. 402-11.
19. Hoffman, S.M., et al., *Endoplasmic reticulum stress mediates house dust mite-induced airway epithelial apoptosis and fibrosis.* Respir Res, 2013. **14**: p. 141.
20. Dunn, K.W., M.M. Kamocka, and J.H. McDonald, *A practical guide to evaluating colocalization in biological microscopy.* Am J Physiol Cell Physiol, 2011. **300**(4): p. C723-42.
21. Vlahopoulos, S., et al., *Nuclear factor-kappaB-dependent induction of interleukin-8 gene expression by tumor necrosis factor alpha: evidence for an antioxidant sensitive activating pathway distinct from nuclear translocation.* Blood, 1999. **94**(6): p. 1878-89.
22. Dinarello, C.A., *Role of pro- and anti-inflammatory cytokines during inflammation: experimental and clinical findings.* J Biol Regul Homeost Agents, 1997. **11**(3): p. 91-103.
23. Roberson, E.C., et al., *Influenza induces endoplasmic reticulum stress, caspase-12-dependent apoptosis, and c-Jun N-terminal kinase-mediated transforming growth factor-beta release in lung epithelial cells.* Am J Respir Cell Mol Biol, 2012. **46**(5): p. 573-81.
24. Kim, S.R. and Y.C. Lee, *Endoplasmic reticulum stress and the related signaling networks in severe asthma.* Allergy Asthma Immunol Res, 2015. **7**(2): p. 106-17.
25. Karbowski, M. and R.J. Youle, *Dynamics of mitochondrial morphology in healthy cells and during apoptosis.* Cell Death Differ, 2003. **10**(8): p. 870-80.